eJSE International

Electronic Journal of Structural Engineering 21 (1) 2021

Condition Assessment of a Reinforced Concrete Residential Building using Non-destructive Testing Methods - A Case Study

Manoj Kumar Rath*

Department of civil engineering, EAST, Bhubaneswar, Odisha India

**Corresponding authors: manojrat@yahoo.com*

ABSTRACT

The present study deals with both experimental and numerical investigation on buckling effects of laminated composite plates subjected to varying temperature and moisture. A simple laminated plate model is developed for the buckling of composite plates subjected to adverse hygrothermal loading. A computer program based on FEM in MATLAB environment is developed to perform all necessary computations. The woven fiber Glass/Epoxy specimens were hygrothermally conditioned in a humidity cabinet where the conditions were maintained at temperatures of 300K-425K and relative humidity (RH) ranging from 0-1% for moisture concentrations. All the investigations are made with a symmetric cross-ply laminates. The present study deals with both experimental and numerical investigation on buckling behavior of laminated composite plates subjected to varying temperature and moisture concentration. Quantitative results are presented to show the effects of geometry, material and lamination parameters of woven fiber laminate on buckling of composite plates for different temperature and moisture concentrations with simply supported boundary conditions with different aspect and side-to-thickness ratios. Experimental results show that there is reduction in buckling loads in KN with the increase in temperature and moisture concentration for laminates with clamped-free-clamped-free boundary conditions

Key words: Adverse hygrothermal environment, Buckling, Woven fiber, Finite element method, Composite plate, Critical load

1. INTRODUCTION

Fiber reinforced plastic composites are being increasingly used in the aerospace industry because of their properties, namely high specific strength, high specific stiffness and low specific density. They are subjected to environmental conditions during their service life. In primary structures is degradation in performance when exposed to a hygrothermal environment. Main aspects of this problem are the reduction in applied loading necessary to buckle composite structures due to these hygrothermal effects. The influences of hygrothermal environment on the elastic stability analysis are

(1) Absorbed moisture causes degradation of matrix dominated mechanical properties at elevated temperatures by reducing the resin's glass transition temperature and modulus by plasticization.
(2) Hygrothermal expansion induces, under certain boundary conditions, significant compressive biaxial stress resultants.

Torabizadeh (2015) an analytical and numerical solution for general laminated composite plates under mechanical loading is presented based on different lamination plate theories. Rhead *et al*. (2017) studied compressive strength of composite laminates with delaminated-induced interaction of panel for sublimate of buckling load. Al-Waily (2020) an analytical investigation of thermal buckling behavior of composite plates is being carried out experimentally. Kolvik and Hellesland (2013) investigated the plate buckling analysis using a general higher-order shear deformation theory.

Abdoun and Azrar (2020) Thermal buckling of laminated composite plates with temperature dependent properties are investigated by using finite element methods. Shojaee *et al*. (2019) studied the post buckling analysis of laminated composites with cut out using experimental by numerical and finite strip methods. Peyyala and Subbarao (2019) presented the polymer laminated composite plates by using shear deformation based on micromechanics model structures with nano carbon tubes. Singh and Chakrabarti (2012) studied the buckling analysis of laminated composite plates using an efficient C^0 finite element model. Croll and Wang (2017) analysed the buckling resistance of fundamental aspect approach referred to reduced stiffness method of the various shell membrane for bending stiffness components. Osman and Suleiman (2017) analyse the buckling analysis of thin laminated composite plates using finite element method

Sai Ram and Sinha (1992) investigated the effects of moisture and temperature on the buckling of laminated composite plates using finite element method. Babu and Kant (2000) proposed with a refined higher order finite element models for buckling of laminated composite and sandwich plates. Spallino and Thierauf (2000) presented the thermal buckling optimization of laminated composite plates subjected to rise in temperature using evolution strategies and a guided random-search method. Shen (2000) examined the influence of hygrothermal effects on the post buckling of shear deformable laminated plates subjected to uniaxial compression using a micro-to-macro-mechanical analytical model of a laminate. Zenkour and EL-Sheikh (2001) presented the buckling of anisotropic elastic plates analytically using simple and mixed shear deformation theories for various boundary conditions. Patel *et al*. (2002) studied the static and dynamic characteristics of thick composite laminates exposed to hygrothermal environment using a higher-order finite element method. Xiao and Chen (2005) studied the dynamic and buckling analysis of a thin elastic-plastic square plate in uniform temperature field using Hamilton's Variational Principle. Jones (2005) studied the thermal buckling of uniformly heated unidirectional and symmetric cross-ply laminated fiber-reinforced composites uniaxial in-plane restrained simply supported rectangular plates. Shariyat (2007) examined the thermal buckling analysis of rectangular composite multilayered plates under uniform temperature rise using a layerwise plate theory and von Karman strain-displacement equations. Matsunaga (2007) studied the free vibration and stability problems of angle-ply laminated composite and sandwich plates subjected to thermal loading using the method of power series expansion. Singh and Verma (2008) investigated the hygrothermal effects on the buckling of laminated composite plates with random geometric and material properties using finite element method. Kumar and Singh (2008) presented the thermal buckling analysis of laminated composite plates subjected to uniform temperature distribution using finite element method. Lal *et al.* (2009) examined the effects of random system properties on thermal buckling load of laminated composite plates under uniform temperature rise using finite element method. Brischetto (2009) studied the thermal stress problem of thick and thin multilayered carbon fiber reinforced cylindrical and spherical shells using Fourier's heat conduction equation. Lal and Singh (2010) presented the effect uncertain system properties thermo-elastic stability of laminated composite plates under nonuniform temperature distribution using A C^0 finite element method. Zenkour (2010) investigated the effect of transverse shear and normal deformations of the thermo mechanical bending of functionally graded sandwich plates using the refined sinusoidal shear deformation plate theory. Pandey *et al.* (2010) observed the effects of moisture and temperature on the post buckling response of a laminated composite plate subjected to hygrother-momechanical loadings using finite double Chebyshev series. Dash *et al.* (2011) presented an experimental study on the elastic buckling and post buckling response of unidirectional E-glass/ epoxy composite rectangular plates subjected to compressive load and liquid environment exposure.

However, in most of the above-mentioned studies on buckling analysis of unidirectional composite plates in hygrothermal environment are reported. But the buckling analysis of woven fiber laminated composite plates in hygrothermal environment is scarce in literature. To the best of author's knowledge, no experimental work is reported in literature on buckling analysis of industry driven woven fiber composite plates subjected to hygrothermal environments.

The present study deals with the parametric study on buckling analysis of woven fiber laminated composite plates subjected to uniform temperature and moisture experimentally and comparing them using finite element method. This paper investigates the effects of aspect ratios, side to thickness ratios, geometry, and lamination parameter on the buckling analysis of simply supported laminated composite plates in adverse hygrothermal environments.

2. MATHEMATICAL FORMULATION

The mathematical formulation for buckling effects of laminated composite plates subjected to moisture and temperature are presented. Consider a laminated plate of uniform thickness ‘t’ consisting of a number of thin lamiae, each of which may be arbitrarily oriented at an angle ‘θ’ with reference to the X-axis of the co-ordinate system as shown in Figures 1 and 2.

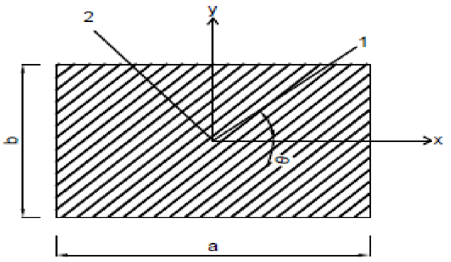

Fig.1. Arbitrarily oriented laminated plate

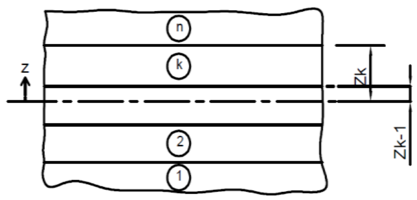

Fig.2. Geometry of an n- layered laminate

2.1. Constitutive Relations

The Constitutive relations for the plate subjected to moisture and temperature are:

$$\{F\}=[D]\{\varepsilon\}-\{F^N\} \tag{1}$$

$$\{F\}=\{N_x,N_y,N_{xy},M_x,M_y,M_{xy},Q_x,Q_y\}^T$$
$$\{F^N\}=\{N_x{}^N,N_y{}^N,N_{xy},M_x{}^N,M_y{}^N,M_{xy}{}^N,0,0\}^T$$
$$\{\varepsilon\}=\{\varepsilon_x,\varepsilon_y,\gamma_{xy},K_x,K_y,K_{xy},\varphi_x,\varphi_y\}^T$$

Where,

Where;

$N_x,N_y,N_{xy}=$ in-plane internal stress resultants.

$M_x,M_y,M_{xy}=$ internal moment resultants.

Q_x,Q_y = transverse shear resultants.

$N_x{}^N,N_y{}^N,N_{xy}{}^N=$ in- plane non-mechanical stress resultants due to moisture and temperature.

$M_x{}^N,M_y{}^N,M_{xy}{}^N=$ non- mechanical moment resultants due to moisture and temperature.

$\varepsilon_x,\varepsilon_y,\gamma_{xy}$ = in-plane strains of the mid-plane.

K_x,K_Y,K_{xy} = Curvature of the plate

φ_x,ϕ_y = Shear rotations in x-z and y-z planes, respectively.

The non-mechanical force and moment resultants due to moisture and temperature are expressed as follows.

$$\{N_x{}^N,N_y{}^N,N_{xy}{}^N\}^T=\sum_{K=1}^{n}\left(\overline{Q_{ij}}\right)\{e\}_k\left(z_k-z_{k-1}\right)$$

For i,j = 1, 2, 6 (2)

$$\{M_x{}^N,M_y{}^N,M_{xy}{}^N\}^T=\frac{1}{2}\sum_{K=1}^{n}\left(\overline{Q_{ij}}\right)_k\{e\}_k\left(z_k{}^2-z_{k-1}{}^2\right)$$

For i,j = 1, 2, 6 (3)

Where

$$\{\varepsilon\}_N=\{\varepsilon_{xN},\varepsilon_{yN},\varepsilon_{xyN}\}^T=[T]\{\beta_1\beta_2\}_k{}^T(C-C_O)+[T]\{\alpha_1\alpha_2\}_k{}^T(T-T_O) \tag{4}$$

In which, $[T]$= Transformation matrix due to moisture and temperature and is given as:

$$[T]=\begin{bmatrix}\cos^2\theta & \sin^2\theta\\ \sin^2\theta & \cos^2\theta\\ \sin 2\theta & \cos 2\theta\end{bmatrix}$$

$\varepsilon_{xN},\varepsilon_{yN},\varepsilon_{xyN}$ = non-mechanical strains due to moisture and temperature

β_1,β_2= moisture coefficient along 1 and 2 axes of lamina, respectively

$\alpha_1.\alpha_2$ = thermal coefficients along 1 and 2 axes of lamina, respectively

T,T_O =Elevated and reference moisture concentration

The stiffness coefficient is defined as:

$$\left(A_{ij}, B_{ij}, D_{ij}\right) = \sum_{k=1}^{n} \int_{z_{k-1}}^{k} \left[Q_{ij}\right]_k \left(1, z, z^2\right) \mathrm{d}z$$

(i, j =1.2.6) (5)

$$S_{ij} = \kappa \sum_{k=1}^{n} \left[Q_{ij}\right]_k dz \qquad \text{(i, j =4,5)}$$

κ = shear correction factor

S_{ij}, B_{ij}, D_{ij} are the extensional, bending-stretching coupling and bending stiffnessess

$\left(\overline{Q_{ij}}\right)_k$ in equations 11 and 12 is defined as:

$$[\overline{Q_{ij}}]_k = [T_1]^{-1}[Q_{ij}]_k [T_1]^{-T}$$

$(i, j = 1, 2, 6)$ (6)

$$\left[\overline{Q}_{ij}\right]_k = [T_2]^{-1}[Q_{ij}]_k [T_2] \qquad (i, j = 4, 5)$$

Where

$$Q_{11} = \frac{E_{11}}{(1-\nu_{12}\nu_{21})}, Q_{12} = \frac{E_{11}\nu_{21}}{(1-\nu_{12}\nu_{21})}, Q_{21} = \frac{E_{22}\nu_{12}}{(1-\nu_{12}\nu_{21})},$$
$$Q_{22} = \frac{E_{22}}{(1-\nu_{12}\nu_{21})}, Q_{66} = G_{12}$$

E_{11}, E_{22} = Young's moduli of a lamina along and across the fibers, respectively

G_{12}, G_{13}, G_{23} = Shear moduli of a lamina with respect to 1, 2 and 3 axes

ν_{12}, ν_{21} = Poisson's ratios

2.2. Strain Displacement Relations

The linear strains are defined as follows

$$\varepsilon_x = \frac{\partial u}{\partial x} + z\kappa_x, \varepsilon_y = \frac{\partial v}{\partial y} + z\kappa_y, \gamma_{xy} = \frac{\partial u}{\partial y} + \frac{\partial v}{\partial x} + z\kappa_{xy}$$
$$\kappa_x = \frac{\partial \theta_x}{\partial x}, \kappa_y = \frac{\partial \theta_y}{\partial y}, \kappa_{xy} = \frac{\partial \theta_x}{\partial y} + \frac{\partial \theta_y}{\partial x}$$

$$\gamma_{xz} = \theta_x + \frac{\partial w}{\partial x}, \gamma_{yz} = \theta_y + \frac{\partial w}{\partial y} \qquad (7)$$

The nonlinear strain components are defined as follows:

$$\varepsilon_{xnl} = \frac{1}{2}\left(\frac{\partial u}{\partial x}\right)^2 + \frac{1}{2}\left(\frac{\partial v}{\partial x}\right)^2 + \frac{1}{2}\left(\frac{\partial w}{\partial x}\right)^2 + \frac{1}{2}z^2\left[\left(\frac{\partial \theta_x}{\partial x}\right)^2 + \left(\frac{\partial \theta_y}{\partial x}\right)^2\right]$$

$$\varepsilon_{ynl} = \frac{1}{2}\left(\frac{\partial u}{\partial y}\right)^2 + \frac{1}{2}\left(\frac{\partial v}{\partial y}\right)^2 + \frac{1}{2}\left(\frac{\partial w}{\partial y}\right)^2 + \frac{1}{2}z^2\left[\left(\frac{\partial \theta_x}{\partial y}\right)^2 + \left(\frac{\partial \theta_y}{\partial y}\right)^2\right]$$

(8)

$$\gamma_{xnl} = \left(\frac{\partial u}{\partial x}\right)\left(\frac{\partial u}{\partial y}\right) + \left(\frac{\partial v}{\partial x}\right)\left(\frac{\partial v}{\partial y}\right) + \left(\frac{\partial w}{\partial x}\right)\left(\frac{\partial w}{\partial y}\right) + z^2\left[\left(\frac{\partial \theta_x}{\partial x}\right)\left(\frac{\partial \theta_y}{\partial y}\right) + \left(\frac{\partial \theta_y}{\partial x}\right)\left(\frac{\partial \theta_x}{\partial y}\right)\right]$$

Green's nonlinear strains are used for derivation of geometrics stiffness matrix due to hygrothermal loads.
u, v, w = displacements of the mid-plane along x, y and z axes respectively
θ_x, θ_y = rotations of the plate about x and y axes

2.3. Finite Element Formulation

An 8-node isoparametric element is used for static stability analysis of woven fiber composite plates subjected to adverse hygrothermal environment. Five degrees of freedom u, v, w, θ_x and θ_y are considered at each node. The stiffness matrix, geometric stiffness matrix due to residual stresses, geometric stiffness matrix due to applied in-plane loads and nodal load vector of the element are derived using the principle of minimum potential energy. The shape function of the element is derived using the interpolation polynomial given below based on Pascal's triangle for convergence criteria.

$$u(\xi,\eta) = a_1 + a_2\xi + a_3\eta + a_4\xi^2 + a_5\xi\eta + a_6\eta^2 + a_7\xi^2\eta + a_8\xi\eta^2 \qquad (9)$$

The displacements are expressed in terms of their nodal values by using the element shape functions and are given by.

$$u = \sum_{i=1}^{8} N_i u_i, v = \sum_{i=1}^{8} N_i v_i, w = \sum_{i=1}^{8} N_i w_i$$
$$\theta_x = \sum_{i=1}^{8} N_i \theta_{xi}, \theta_y = \sum_{i=1}^{8} N_i \theta_{yi} \qquad (10)$$

The shape function N_i are defined as;

$$N_i = \frac{1}{4}(1+\xi\xi_i)(1+\eta\eta_1)(\xi\xi_1+\eta\eta_1-1)$$

For $i = 1, 2, 3$ & 4

$$N_i = \frac{1}{2}(1-\xi^2)(1+\eta\eta_i) \qquad \text{For } i = 5, 7$$

$$N_i = \frac{1}{2}(1-\xi\xi_i)(1-\eta^2) \qquad \text{For } i = 6, 8$$

$\xi, \eta =$ Local natural co-ordinates of an element

$N_i =$ Shape function at a node i

2.4. Element stiffness matrix

The linear strain matrix $\{\varepsilon\}$ is expressed as:

$$\{\varepsilon\} = [B]\{\delta_e\} \tag{11}$$

Where

$$\{\delta_e\} = \{u_1, v_1, w, \theta_{x1}, \theta_{y1} \ldots\ldots\ldots, u_8, v_8, w_8 \theta_{x8}, \theta_{y8}\}^T,$$

$$[B] = \sum_{i=1}^{8} \begin{bmatrix} N_{i,x} & 0 & 0 & 0 & 0 \\ 0 & N_{i,y} & 0 & 0 & 0 \\ N_{i,y} & N_{i,x} & 0 & 0 & 0 \\ 0 & 0 & 0 & 0 & N_{i,x} \\ 0 & 0 & 0 & N_{i,y} & 0 \\ 0 & 0 & 0 & N_{i,x} & N_{i,y} \\ 0 & 0 & N_{i,x} & 0 & N_i \\ 0 & 0 & N_{i,y} & N_i & 0 \end{bmatrix}$$

Element stiffness matrix is given by

$$[K_e] = \int_{-1}^{+1}\int_{-1}^{+1} [B]^T [D][B] |J| \, d\xi \, d\eta \tag{12}$$

2.5. Geometric stiffness matrix $[K^r{}_{Ge}]$

The non-linear strain equations are represented in matrix form:

$$\varepsilon_{nl} = \{\varepsilon_{xnl}, \varepsilon_{ynl}, \gamma_{xynl}, \gamma_{xznl}, \gamma_{yznl}\}^T = [R]\{d\}/2$$

(13)

Where

$$\{d\} = \{u_x, u_y, v_x, v_y, w_x, w_y, \theta_{x,x}, \theta_{x,y}, \theta_{y,x}, \theta_{y,y}, \theta_x, \theta_y\}^T$$

Equations $\{d\}$ may be expressed as:

$$\{d\} = \{G\}\{\partial_e\} \tag{14}$$

Where

$$[G] = \sum_{i=1}^{8} \begin{bmatrix} N_{i,x} & 0 & 0 & 0 & 0 \\ N_{i,y} & 0 & 0 & 0 & 0 \\ 0 & N_{i,x} & 0 & 0 & 0 \\ 0 & N_{i,y} & 0 & 0 & 0 \\ 0 & 0 & N_{i,x} & 0 & 0 \\ 0 & 0 & N_{i,y} & 0 & 0 \\ 0 & 0 & 0 & N_{i,x} & 0 \\ 0 & 0 & 0 & N_{i,y} & 0 \\ 0 & 0 & 0 & 0 & N_{i,x} \\ 0 & 0 & 0 & 0 & N_{i,y} \\ 0 & 0 & 0 & 1 & 0 \\ 0 & 0 & 0 & 0 & 1 \end{bmatrix}$$

The geometric stiffness matrix due to residual stresses is given by

$$[K^r{}_{Ge}] = \int_{-1}^{+1}\int_{-1}^{+1} [G]^T [S][G] |J| \, d\xi \, d\eta \tag{15}$$

Where

$$[S] = \left[0 \; \begin{matrix} S_{11} & & & & & & & & & & & \\ S_{21} & S_{22} & & & & & & & & & & \\ 0 & 0 & S_{33} & & & & & & & & & \\ 0 & 0 & S_{43} & S_{44} & & & & & & & & \\ 0 & 0 & 0 & 0 & S_{55} & & & & & & & \\ 0 & 0 & 0 & 0 & S_{65} & S_{66} & & & & & & \\ 0 & 0 & S_{73} & S_{74} & 0 & 0 & S_{77} & & & & & \\ 0 & 0 & S_{83} & S_{84} & 0 & 0 & S_{87} & S_{88} & & & & \\ S_{91} & S_{92} & 0 & 0 & 0 & 0 & 0 & 0 & S_{99} & & & \\ S_{101} & S_{102} & 0 & 0 & 0 & 0 & 0 & & S_{109} & S_{110} & & \\ 0 & 0 & S_{113} & S_{114} & 0 & 0 & 0 & 0 & 0 & 0 & 0 & \\ S_{121} & S_{122} & 0 & 0 & 0 & 0 & 0 & 0 & 0 & 0 & 0 & 0 \end{matrix} \right]$$

In which

$$S_{11} = S_{33} = S_{55} = N^r{}_x$$

$$S_{21} = S_{43} = S_{65} = N^r{}_{xy},$$

$$S_{22} = S_{44} = S_{66} = N^r{}_y$$

$$S_{77} = S_{99} = N_x{}^r \; t^2/12$$

$$S_{87} = S_{109} = N^r{}_{xy} t^2/12$$

$$S_{88} = S_{1010} = N_y{}^r \; t^2/12$$

$$-S_{73} = S_{91} = M^r{}_x$$

$-S_{84} = S_{102} = M^r{}_y$

$-S_{74} = -S_{83} = S_{92} = S_{101} = M^r{}_{xy}$

$-S_{113} = S_{121} = Q^r{}_x$

$-S_{114} = S_{122} = Q^r{}_y$

$N^{ir}{}_x, N^r{}_y, N^r{}_{xy} =$ in-plane initial internal force resultants per unit length

$M^r{}_x, M^r{}_y, M^r{}_{xy} =$ initial internal moment resultants per unit length

$Q^r{}_x, Q^r{}_y =$ initial transverse shear resultants

2.6. Geometric stiffness matrix $\left[K^a{}_{Ge}\right]$

The first three non-linear strain equations are represented in a matrix form:

$$\{\varepsilon_{xnl}, \varepsilon_{ynl}, \gamma_{xynl}\}^T = [U]\{f\}/2 \tag{16}$$

$$\{f\} = \{u_x, u_y, v_x, v_y, w_x, w_y, \theta_{x,x}, \theta_{x,y}, \theta_{y,x}, \theta_{y,y}\}^T$$

$\{f\}$ is expressed as:

$$\{f\} = [H]\{\delta_e\} \tag{17}$$

Where

$$[H] = \sum_{i=1}^{8} \begin{bmatrix} N_{i,x} & 0 & 0 & 0 & 0 \\ N_{i,y} & 0 & 0 & 0 & 0 \\ 0 & N_{i,x} & 0 & 0 & 0 \\ 0 & N_{i,y} & 0 & 0 & 0 \\ 0 & 0 & N_{i,x} & 0 & 0 \\ 0 & 0 & N_{i,y} & 0 & 0 \\ 0 & 0 & 0 & N_{i,x} & 0 \\ 0 & 0 & 0 & N_{i,y} & 0 \\ 0 & 0 & 0 & 0 & N_{i,x} \\ 0 & 0 & 0 & 0 & N_{i,y} \end{bmatrix}$$

The geometric stiffness matrix due to applied in-plane loads is given by

$$\left[K^a{}_{Ge}\right] = \int_{-1}^{+1}\int_{-1}^{+1} [H]^T [P][H] |J| d\xi d\eta \tag{18}$$

Where

$$[P] = \begin{bmatrix} P_{11} & & & & & & & & & \\ P_{21} & P_{22} & & & & & & & & \\ 0 & 0 & P_{33} & & & & & & & \\ 0 & 0 & 0 & P_{44} & & & & & & \\ 0 & 0 & 0 & 0 & P_{55} & & & & & \\ 0 & 0 & 0 & 0 & P_{65} & P_{66} & & & & \\ 0 & 0 & 0 & 0 & 0 & 0 & P_{77} & & & \\ 0 & 0 & 0 & 0 & 0 & 0 & P_{87} & P_{88} & & \\ 0 & 0 & 0 & 0 & 0 & 0 & 0 & 0 & P_{99} & \\ 0 & 0 & 0 & 0 & 0 & 0 & 0 & 0 & P_{109} & P_{1010} \end{bmatrix}$$

In which

$P_{11} = P_{33} = P_{55} = N^a{}_x$

$P_{21} = P_{43} = P_{65} = N^a{}_{xy}$

$P_{22} = P_{44} = P_{66} = N^a{}_y \qquad P_{77} = P_{99} = N^a{}_x t^2/12$

$P_{88} = P_{1010} = N^a{}_y t^2/12 \qquad P_{87} = P_{109} = N^a{}_{xy} t^2/12$

$N^a{}_x, N^a{}_y, N^a{}_{xy} =$ Applied in-plane forces per unit length

2.7. Load vector

The element load vector due to the hygrothermal forces and moments is given by

$$\{P^N\} = \int_{-1}^{+1}\int_{-1}^{+1} [B]^T \{F^N\} |J| d\xi d\eta \tag{19}$$

2.8. Solution process

The stiffness matrix, the initial stress stiffness matrix due to hygrothermal load, the geometric stiffness matrix and the load vectors of the element, given by equations (9)-(15), are evaluated by first expressing the integrals in local Natural co-ordinates, ξ and η of the element and then performing numerical integration by using Gaussian quadrature. Then the element matrices are assembled to obtain the respective global matrices $[K]$, $\left[K^r{}_{Ge}\right]$, $\left[K^a{}_{Ge}\right]$ and $\{P^N\}$. The first part of the solution is to obtain the initial stress resultants induced by the moisture and temperature conditions.

The initial displacements $\{\delta^i\}$, are found the equilibrium condition

For buckling $\qquad [K]\{\delta^i\} = \{P^N\} \qquad (20)$

Then the initial stress resultants

$N^i{}_x, N_y{}^i, N^i{}_{xy}, M^i{}_x, M^i{}_y, M^i{}_{xy}, Q^i{}_x$ and $Q^i{}_y$ are obtained from equations (1) and (10). The second part of the solution involves determination of natural frequencies from the conditions given below

Critical loads

$$[K]+[K^r{}_{Ge}]-\lambda[K^a{}_{Ge}] \tag{21}$$

λ = Critical loads

3. EXPERIMENTAL PROGRAMME

Glass fiber: epoxy composite specimens were fabricated using weight fraction of 55:45 by hand layup method. Woven roving E-Glass fibers (FGP, RP-10) were cut into required size according to number of specimens required for testing. Each composite laminates consists of 16 plies of fiber in balanced form as per ASTM specification. For preparation of Epoxy resin matrix, Hardener 8% (Ciba-Geigy, araldite LY556 and Hardener HY951) of the weight of Epoxy was used as per ASTM D5687/D5687M-07. A flat plywood rigid platform was selected. A plastic sheet i.e. a mould releasing sheet was kept on the plywood platform and a thin film of polyvinyl alcohol was applied as a releasing agent. Laminating was done with the application of a gel coat (Epoxy and hardener) deposited on the mould by brush, whose main purpose was to provide a smooth external surface and to protect the fibers from direct exposure to the environment. Layers of reinforcement were placed on the mould at top of the gel coat and gel coat was applied again by brush. Any air which may be entrapped was removed using serrated steel rollers to minimize void contents in the samples. The process of hand lay-up was the continuation of the above process before the gel coat had fully hardened. After completion of all the layers, again a plastic sheet was covered at the top of last ply by applying polyvinyl alcohol inside the sheet as a releasing agent. Again one flat ply board and a heavy flat metal rigid platform were kept on top of the plate for compressing purpose. The laminates were cured at normal temperature (25^0C and 55 % Relative Humidity) under a pressure of 0.2 Ma for 3 days. After proper curing of laminates, the release film was detached. The specimens were cut for buckling testing by brick cutting machine into 235mm×235mm. The thickness of 16 layer laminate was measured as 6.0 mm.

3.1. Hygrothermal treatment

The specimens were hygrothermally conditioned in a humidity cabinet as shown in figure 3, where the conditions were maintained at a temperature of 323K and relative humidity (RH) ranging from 0-1% for moisture concentration as per ASTM D5229/ D5229M-04. The humidity cabinet had an inbuilt thermometer for temperature and hygrometer for relative humidity measurements. The temperature variation was maintained between 300K-425K whereas the RH was 0 in temperature bath as shown in figure 4. The composite laminates were placed on perforated trays.

Fig.3. Humidity chamber

Fig.4.TemperatureBath

3.2. Buckling Experiment

In view of difficulty of theoretical and numerical analysis for laminated structure behaviors, experimental methods have become important in solving the buckling problem of laminated composite plates. The specimen was clamped at two sides and kept free at two other sides. The specimen was loaded in axial compression by using an INSTRON 1195 Machine of 600 KN load capacity as shown in figure 5. All specimens were loaded slowly unless buckling takes place. Clamped boundary conditions were simulated along top and bottom edges, restraining 2.5cm length. For axial loading, the test specimens were placed between the two extremely stiff machine heads, of which the lower one was fixed during the test; whereas the upper head was moved downwards by servo hydraulic cylinder. All plates were loaded at constant cross-head speed of 0.5mm/min. The shape of the specimen after buckling is as shown in figure 6. The load verses end shortening curve was plotted. The displacement is plotted along x-axis and the load was plotted on the y-axis. The load, which is the initial part of the curve deviated linearity, is taken as the critical buckling load in kN.

Fig.5.Instron-1195 machine with specimen

Fig.6. Specimen after buckling

4. RESULTS AND DISCUSSION

The results of buckling effects of woven fiber composite plates subjected to hygrothermal loadings are presented using the above formulations. The results are presented as follows:

- Convergence study
- Comparison with previous studies
- New results

4.1. Convergence study

The convergence study is first done for non-dimensional frequencies of free vibration of 4 layer symmetric cross-ply and symmetric angle-ply laminated composite plates and for non-dimensional critical load at a temperature of 325K and 0.1% moisture concentration for different mesh divisions is shown in Table 1, 2, 3, 4 respectively. As observed, a mesh of 10 ×10 shows good convergence of the numerical solution for the free vibration and buckling analysis of woven fiber composite plates in hygrothermal environment and this mesh is employed throughout for free vibration and buckling analysis of woven fiber composite plates in hygrothermal environment.

Table 1. Convergence of non-dimensional fundamental frequencies of free vibration for SSSS four layered laminated composite plates for two different lamination sequences at 325K temperature

a/b =1, a/t= 100, At T=300K, E_1=130GPa, E_2=9.5Gpa, G_{12}=6GPa, $G_{13}=G_{12}$, $G_{23}=0.5G_{12}$, ν_{12}=0.3 α_1=-0.3 X $10^{-6}/^{O}$K, α_2 =28.1 X $10^{-6}/^{O}$K

Non dimensional frequency, $\lambda = \omega_n a^2 \sqrt{\rho / E_2 t^2}$

Mess Division	Non- dimensional frequencies at 325K Temperature	
	0/90/90/0	45/-45/-45/45
4x4	8.079	11.380
6x6	8.039	10.785
8x8	8.036	10.680
10x10	8.036	10.680

Table 2. Convergence of non-dimensional fundamental frequencies of free vibration for SSSS four layered laminated composite plates for two different lamination sequences at 0.1% moisture concentration.

a/b =1, a/t= 100, At T=300K, E_1=130GPa, E_2=9.5GPa, G_{12}=6GPa, $G_{13}=G_{12}$, $G_{23}=0.5G_{12}$, ν_{12}=0.3 β_1=0, β_2=0.44

Non dimensional frequency, $\lambda = \omega_n a^2 \sqrt{\rho / E_2 t^2}$

Mess Division	Non- dimensional frequencies at 0.1% Moisture concentration	
	0/90/90/0	45/-45/-45/45
4x4	9.422	12.383
6x6	9.387	11.858
8x8	9.384	11.765
10x10	9.384	11.765

Table 3. Convergence of non-dimensional critical load for SSSS four layered laminated composite plates for two different lamination sequences at 325K temperature.

a/b =1, a/t= 100, At T=300K, E_1=130GPa, E_2=9.5GPa, G_{12}=6GPa, $G_{13}=G_{12}$, $G_{23}=0.5G_{12}$, ν_{12}=0.3 α_1=-0.3 X 10^{-6}/^{O}K, α_2 =28.1 X 10^{-6}/^{O}K

Critical load, $\lambda = N_{xcr} / (N_{xcr})_{C=0\%}$ or T =300K

Mess Division	Non- dimensional critical load at 325K Temperature	
	0/90/90/0	45/-45/-45/45
4x4	0.4481	0.6120
6x6	0.4459	0.5818
8x8	0.4457	0.5764
10x10	0.4457	0.5745

Table 4. Convergence of non-dimensional critical load for SSSS four layered laminated composite plates for two different lamination sequences at 0.1% moisture concentration.

a/b =1, a/t= 100, At T=300K, E_1=130GPa, E_2=9.5GPa, G_{12}=6GPa, $G_{13}=G_{12}$, $G_{23}=0.5G_{12}$, ν_{12}=0.3 β_1=0, β_2=0.44

Critical load, $\lambda = N_{xcr} / (N_{xcr})_{C=0\%}$ or T =300K

Mess Division	Non- dimensional critical load at 0.1% Moisture concentration	
	0/90/90/0	45/-45/-45/45
4x4	0.6095	0.7255
6x6	0.6079	0.7041
8x8	0.6078	0.7003
10x10	0.6078	0.7003

4.2. Comparison with previous studies

The results obtained by this present formulation are compared with the analytical results published by the other investigator whenever possible for variety of prolems on plates under hygrothermal environment.

4.2.1. Free vibration of composite plates

The present formulation is validated for free vibration analysis of composite plates for temperature and moisture as shown in Table 5 & Table 6. The square plate has four layers of Graphite / Epoxy composite. The four lowest non-dimensional frequency parameters due to hygrothermal loadings obtained by the present finite element are compared with numerical solution published by Sairam and Sinha [1992] and with those of (Shen, Zheng and Huang 2004) using a micro-to-macro mechanical analytical model. The present finite element result shows good agreement with the previous results published in the literature.

Table 5.Comparison of non-dimensional free vibration frequencies for SSSS (0/90/90/0) plates at 325K temperature

a/b=1, a/t=100, At T = 300*K*, E1= 130GPa, E_2= 9.5GPa, G_{12}= 6GPa, G13=G_{12}, $G_{23}=0.5G_{12}$, ν_{12}=0.3, α_1=-0.3 X 10^{-6}/^{O}K, α_2 =28.1 X 10^{-6}/^{O}K

Non dimensional frequency, $\lambda = \omega_n a^2 \sqrt{\rho / E_2 t^2}$

Non- dimensional frequencies at 325K Temperature			
Mode number	Shen, Zheng and Huang [15]	Sairam & Sinha [14]	Present FEM
1	7.702	8.088	8.079
2	17.658	19.196	19.100
3	38.312	39.324	39.335
4	44.038	45.431	45.350

Table 6. Comparison of non-dimensional free vibration frequencies for SSSS (0/90/90/0) plates at 0.1% moisture concentration a/b=1, a/t=100, At T = 300*K*, E_1= 130GPa , E_2= 9.5GPa, G_{12}= 6GPa , $G_{13}=G_{12}$, $G_{23}=0.5G_{12}$, ν_{12}=0.3, β_1=0, β_2=0.44,

Non dimensional frequency, $\lambda = \omega_n a^2 \sqrt{\rho / E_2 t^2}$

Non- dimensional frequencies at 0.1% Moisture concentration			
Mode number	Shen, Zheng and Huang [15]	Sairam & Sinha [14]	Present FEM
1	9.413	9.429	9.422
2	19.867	20.679	20.597
3	39.277	40.068	40.084
4	45.518	46.752	46.708

4.2.2. Buckling of composite plates

The present formulation is validated for buckling analysis of composite plates for temperature and moisture as shown in Table 7. The square plate has four layers of Graphite / Epoxy composite. The non-dimensional critical load due to hygrothermal loadings obtained by the present finite element is compared with analytical solution published by (Sairam and Sinha 1992) and (Patel, Ganapathi and Makhecha 2002). The present finite element results show good agreement with the previous analytical results published in the literature for buckling of laminated composite plates.

Table 7. Comparison of non-dimensional critical load for SSSS (0/90/90/0) four layered laminated composite plates at 325K temperature and 0.1% moisture concentration.

a/b =1, a/t= 100, At T=300K, E1=130GPa, E2=9.5GPa, G12=6GPa, G13=G12, G23=0.5G12, ν12=0.3 α1=-0.3 X 10-6/OK, α2 =28.1 X 10-6/OK, β1=0, β2=0.44

Non-dimensional Critical load, $\lambda = Nxcr / (Nxcr)_{C=0\%}$ or T =300K

References	Non-dimensional critical load λ	
	At 325K	At 0.1%
Sairam & Sinha [16]	0.4488	0.6099
Patel,Ganapathi & Makhecha [17]	0.4466	0.6084
Present FEM	0.4481	0.6095

4.3. New Results for Critical loads

Numerical results are presented for the buckling effects of woven fiber composite plates in hygrothermal environment. The geometrical and material properties of the laminated composite plates are: a=b=0.235m, h=0.006m (unless otherwise stated). The material properties obtained from tensile testing of glass/epoxy composite plates at different temperatures and moisture as per ASTM D3039/D3039M- 2008 are shown in table 8 and table 9.

Table 8. Elastic moduli of glass fiber/epoxy lamina at different temperatures.(Experimental values)
α_1=-0.3 X $10^{-6}/^{O}$K, α_2 =28.1 X $10^{-6}/^{O}$K, β_1=0, β_2=0.44

	Temperature in (K)					
Elastic moduli	300	325	350	375	400	425
E_1	7.9	7.6	7.1	6.7	6.5	6.3
E_2	7.4	6.8	6.4	6.2	5.9	5.7
G_{12}	1.6	2.9	2.6	2.3	2.1	1.8
ν_{12}	0.4	0.43	0.41	0.35	0.36	0.35

Table 9. Elastic moduli of glass fiber / epoxy lamina at different moisture concentrations. (Experimental values)

α_1=-0.3 X $10^{-6}/^{O}$K, α_2 =28.1 X $10^{-6}/^{O}$K, β_1=0, β_2=0.44

	Moisture concentration in %				
Elastic moduli	0.0	0.25	0.5	0.75	1.0
E_1	7.9	7.6	7.5	7.3	7.2
E_2	7.4	7.4	7.3	7.1	7.0
G_{12}	2.9	2.9	2.8	2.7	2.6
ν_{12}	0.4	0.4	0.4	0.39	0.39

- Experimental results for critical loads
- Ply orientation
- Number of layers
- Aspect ratios
- Side to thickness ratios

The geometrical and non-mechanical properties are:
a=b=235mm, t= 6mm,
Thermal coefficient
α_1=-0.3 X $10^{-6}/^{O}$K, α_2 =28.1 X $10^{-6}/^{O}$K,
Moisture coefficient β_1=0, β_2=0.44
The comparison of results for critical buckling loads in kN of both the numerical analysis and experimental values with increase in temperature from 300K to 425K in every 25K rise in temperature and 0 to 1% in every 0.25% rise in moisture concentration of woven roving glass fiber/epoxy composites are presented for clamped-free-clamped-free boundary condition. The accuracy of the present finite element analysis is verified with the Sai Ram and Sinha method for a $[0/90]_{4S}$ laminate. Lamina material properties at elevated moisture concentrations and temperatures used in the present analysis are shown in Tables 8 and 9. The value of shear correction factor is taken as 5/6. The variation of critical buckling loads with increase in temperature and moisture concentration through the entire volume of the plate is shown graphically in figure 9 and 10. This shows that there is a good agreement between experimental and numerical results. It is observed that increase in temperature and moisture concentration there is a decrease in critical buckling load because of reduction of stiffness and strength. The effect of temperature generally causes a softening of the fibers and the effect of moisture causes plasticization due to absorbed moisture. The critical buckling load decreased severely with temperature beyond 400K and moisture concentration beyond 1%, in which hygrothermal buckling appears. In thermal buckling the composite plate does not remain perfectly flat and suddenly develops a large deformation due to critical temperature stress is reached, the plate will begin to deform as soon as thermal stresses

are developed, the deformation will increase rapidly due to increase in temperature which is known as buckling temperature. The reduction in critical buckling load in kN is more pronounced at higher temperature and moisture is due to working temperature is increased closer to the lowered glass transition temperature at increased moisture concentration. The buckling load is reduced by approximately 27% when the plate is subjected to 1% moisture concentration and temperature increase of 400K in comparison to the buckling load of the plate without hygrothermal loading.

The effects of reduction in the buckling loads in kN are more prominent for temperature as compared to moisture concentration. It clearly demonstrates that the detrimental effect of the increased moisture concentration and temperature on the stability of the plate. It is also seen that the hygroscopic condition on the stability of the plate becomes more significant in presence of the thermal loading. The hygrothermal buckling load in kN decreases and the effects are more prominent for temperature compared to moisture concentrations.

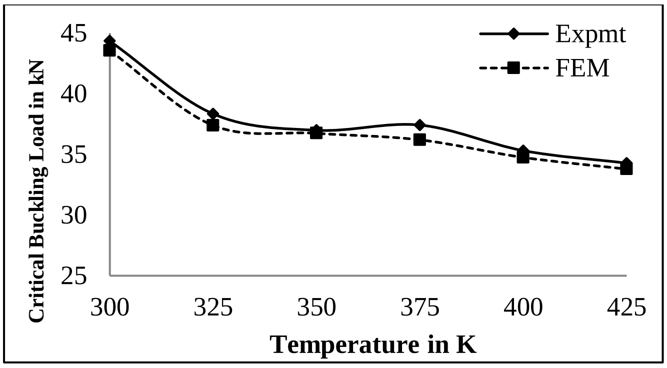

Fig.7. Variation of critical buckling load in kN with temperature of 16 layers $[0/90]_{4S}$ woven fiber laminated composite plates (C-F-C-F)

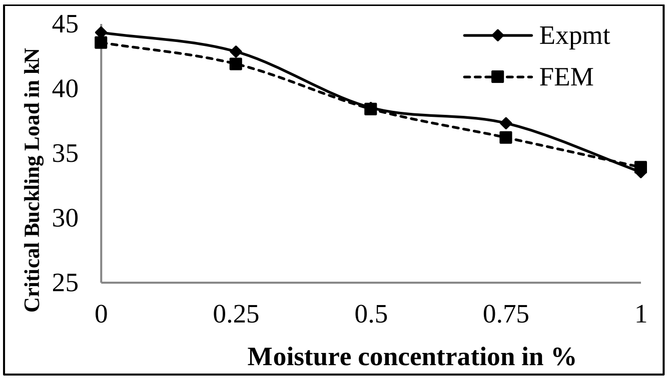

Fig.8. Variation of critical buckling load in kN with moisture concentration of 16 layers [0/90]4S woven fiber laminated composite plates (C-F-C-F)

The variation of critical buckling load in kN for sixteen layers of composite plates with simply supported boundary conditions are presented (a/b=1, a/t=40), subjected to uniform distribution of temperature from 300K to 425K and moisture concentration from 0 to1% with different lamination sequence is shown in figure 11 and 12 respectively. It is shown that the critical buckling loads for anti-symmetric laminates are more as compared to symmetric laminates with increasing in uniform temperature and moisture concentration environment. With increase in temperature the reduction in critical buckling loads is nonlinear but with increase in moisture concentration the reduction in critical buckling loads is linear.

It is observed that this greater reduction in the critical buckling loads in kN is due to the effect of decrease in shear modulus with increase in temperature and moisture concentration. The result shows that decreasing in buckling loads is independent of fiber orientation angle

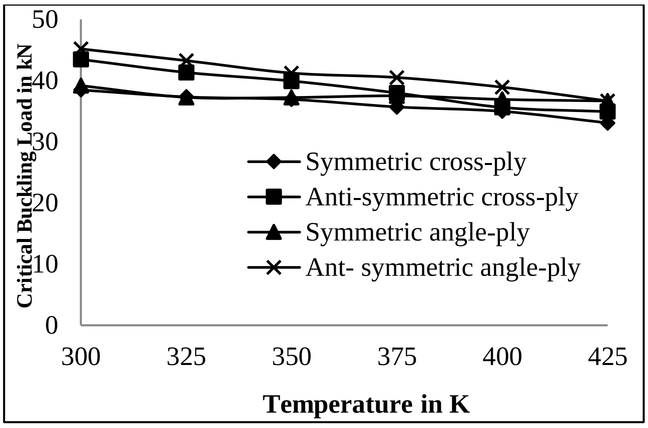

Fig.9. Variation of critical buckling load in kN with temperature of 16 layers [0/90] 4S, [45/-45]4S and [0/90]8, [45/-45]8 woven fiber laminated composite plates (S-S-S-S)

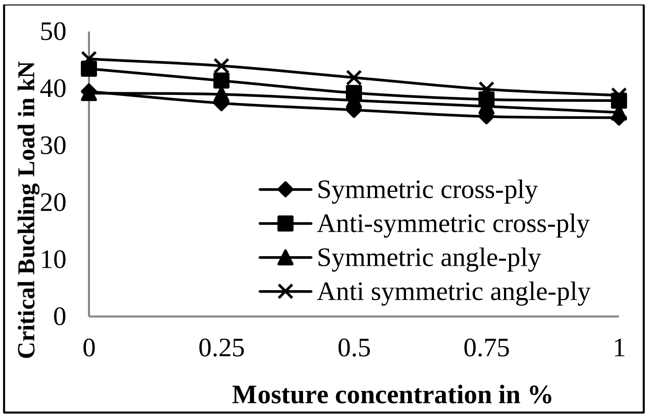

Fig.10. Variation of critical buckling load in kN with moisture concentration of 16 layers [0/90] 4S, [45/-

45]4S and [0/90]8, [45/-45]8 woven fiber laminated composite plates (S-S-S-S)

The variation of critical buckling loads in kN (a/b=1, a/t=40) for eight, twelve and sixteen layers simply supported, cross-ply symmetric laminated plates subjected to uniform distribution of temperature and moisture concentration is shown in figure 13 and 14. It is shown that the reduction in critical buckling loads in kN with uniform increase in temperature and moisture concentration is of the same order for eight, twelve and sixteen layer cross-ply symmetric plates. The critical load remains constant with increasing in number of layers of laminates beyond eight layers. It is also noted that with increase in temperature hardening type nonlinear behavior of the critical loads for all layers of laminates

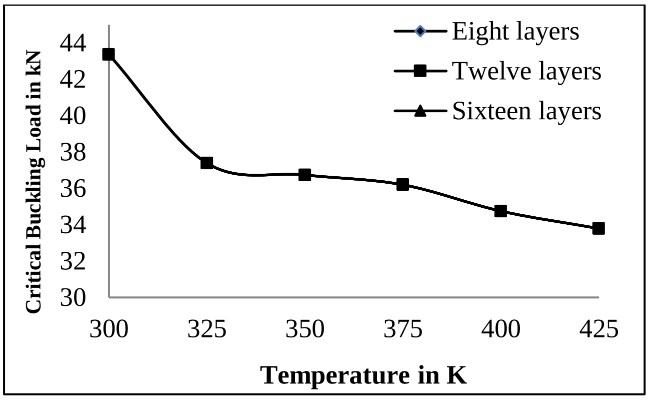

Fig.11. Variation of critical buckling load in kN with temperature of 16 layers $[0/90]_{4S}$, 12 layers $[0/90]_{3S}$, 8 layers $[0/90]_{2S}$ woven fiber laminated composite plates (S-S-S-S)

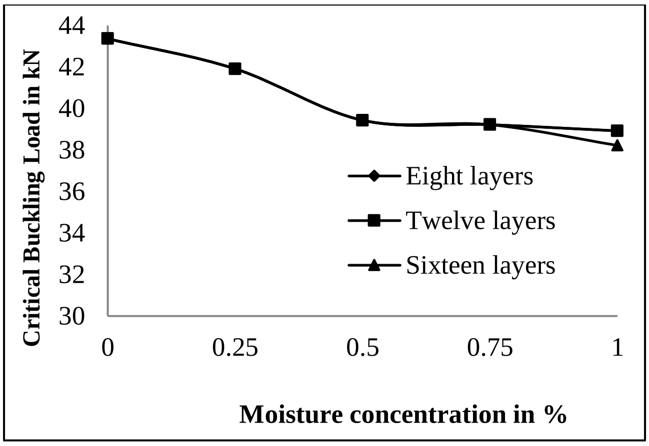

Fig.12. Variation of critical buckling load in kN with moisture concentration of 16 layers $[0/90]_{4S}$, 12 layers $[0/90]_{3S}$, 8 layers $[0/90]_{2S}$ woven fiber laminated composite plates(S-S-S-S)

The variation of critical loads in kN (a/b=0.5, a/b=1 and a/b=2 for a/t=40) for sixteen layers simply supported boundary condition for cross-ply symmetric plates subjected to uniform distribution of temperature and moisture concentration with different aspect ratios is shown in figure 15 and 16. It is shown that the reduction of critical loads with increase in temperature and moisture concentration having aspect ratio 0.5 is more than the aspect ratio 1 and 2. As increase in aspect ratios beyond 1 and above, the critical buckling loads in kN are decreased marginally hygrothermal environment. It is observed that the critical buckling loads in kN is highest for a/b=0.5 and stability decreases with increase in aspect ratios of woven fiber laminated composite plates in hygrothermal environment. For higher buckling load strength corresponding to a/b=1, and 2 is almost same with rise in temperature and moisture concentration. Hygrothermal buckling also starts at room temperature about 300K which is known as stress–free level. Similarly hygroscopic buckling will start at 0.25% of moisture concentration which is also known as stress-free level. As the hygrothermal stress resultants are integrated quantities, their effect increases with the absorption of more moisture until equilibrium is reached.

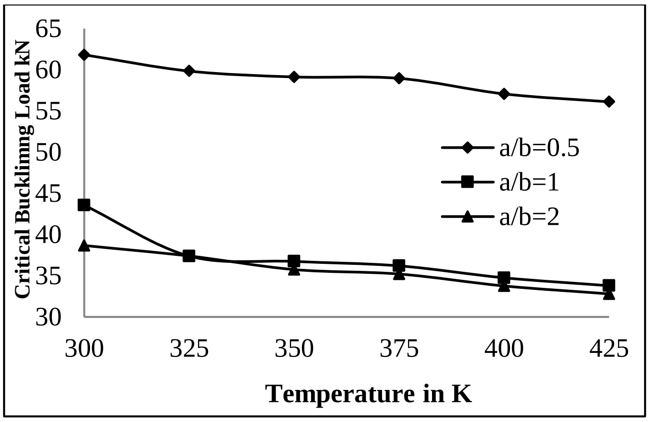

Fig.13. Variation of critical buckling load in kN with temperature of 16 layers $[0/90]_{4S}$ woven fiber laminated composite plates (S-S-S-S)

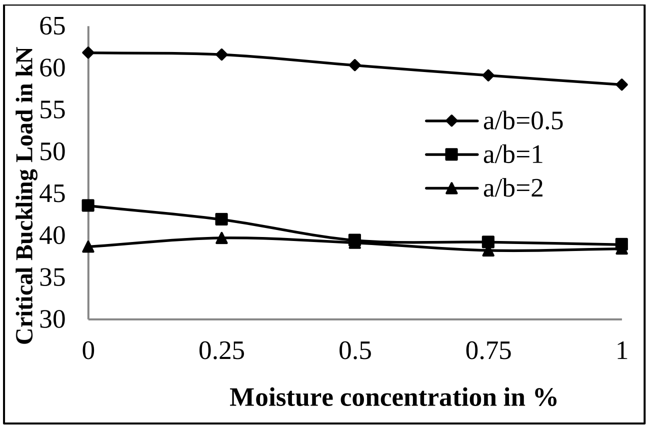

Fig.14. Variation of critical buckling load in kN with moisture concentration of 16 layers $[0/90]_{4S}$ woven fiber laminated composite plates (S-S-S-S)

The variation of critical buckling loads in kN (for a/b=1, a/t=25, a/t=40 and a/t=100) for sixteen layers simply supported boundary conditions for cross-ply symmetric plates subjected to uniform distribution of temperature and moisture concentration with different side to thickness ratios is shown in figure 17 and 18. From the results it is also clear that the reduction in critical buckling loads in kN with increase in temperature and moisture is more for plates with lower side-to-thickness ratios than higher side-to-thickness ratio. This present method of analysis has been found efficient in order to evaluate the critical buckling load in kN of moderately thick composite laminated plate subjected to hygrothermal loading. It is seen that the buckling load in kN decreases with increase in moisture concentration for different aspect and side-to-thickness ratios due to degradation in material properties at higher temperature and moisture concentration. It is also evident from the graph that the thin laminated composite plates are more stable compared to moderately thick plates with increase in temperature and moisture concentration environment. The random changes in thickness have more impact on hygrothermal buckling load scattering compared to individual random changes in material property. The sensitivity of hygrothermal buckling load due to variation in geometric and material properties is dependent on thickness only.

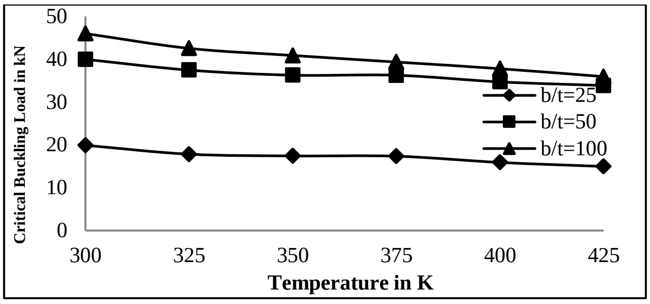

Fig.15. Variation of critical buckling load in kN with temperature of 16 layers $[0/90]_{4S}$ woven fiber laminated composite plates (S-S-S-S)

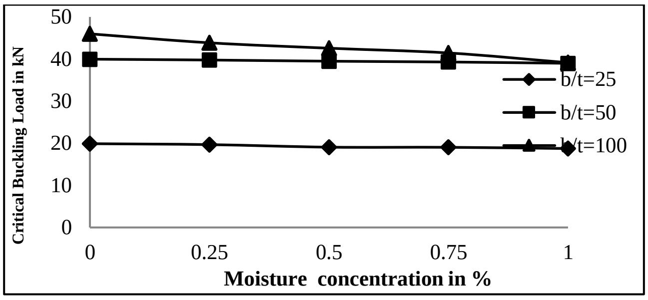

Fig.16. Variation of critical buckling load in kN with moisture concentration of 16 layers $[0/90]_{4S}$ woven fiber laminated composite plates (S-S-S-S)

It is seen that these hygrothermal loads significantly reduce the applied surface tractions necessary to buckle a composite structure with clamped-free-clamped-free and simply supported boundary conditions with increase in temperature and moisture concentration environment.

5. CONCLUSIONS

The present study deals with the parametric study on buckling behavior of woven fiber composite plates subjected to uniform temperature and moisture experimentally and comparing them using finite element method. From the discussion, the following observation can be made:

- There is a good agreement between the experimental and numerical results for buckling of laminated composite plates at different temperature and moisture concentration.
- The critical load in kN decreases with increase in temperature and moisture concentration.
- With increase in temperature the reduction in critical loads is nonlinear.
- With increase in uniform moisture concentration, the reduction in critical load in kN is nearly linear.

- The reduction in critical loads in kN with increase in temperature and moisture concentration is of the same order for eight, twelve and sixteen layers of cross-ply symmetric laminated plates.
- The of critical buckling loads in kN for different lamination sequence is decreased for anti-symmetric laminates compared to symmetric laminates with increase in temperature and moisture concentration.
- The critical load in kN is decreased with increase in aspect ratios with uniform rise in temperature and moisture environment.
- The critical load in kN is increased with increase in side-to-thickness ratio with uniform rise in temperature and moisture concentration.
- The thin laminated composite plates are more stable than moderately thick plates in hygrothermal environment.
- The hygrothermal buckling load is most affected with random changes in E_{22}, while it is least affected with random changes in G_{12}.
- The critical buckling loads in kN may vanish depending upon the temperature, moisture concentration, lamination sequence, side-to-thickness ratios and aspect ratios.
- The clamped-free-clamped-free boundary condition shows better critical buckling loads in kN as compared to four sides simply supported edge.
- From the present studies, it is concluded that the buckling behavior of woven fiber composite plates is greatly influenced by the geometry and lamination parameter. Such a property can be utilized to tailor the design of woven fiber composite plates in adverse hygrothermal environment.

REFERENCES

1. ASTM Standard: D5687/D5687M-07. 2007. "Standard Guide for Preparation of Flat Composite Panels With Processing Guidelines For Specimen Preparation."

2. ASTM Standard: D5229/D5229M-04. 2004. "Stanndard Test Method For Moisture Absorption."

3. ASTM Standard: D3039/D3039M-08. 2008. "Standard Test Method for Tensile Properties of Polymer Matrix Composite Materials."

4. Abdoun, F and Azrar, L (2020) "Thermal buckling and vibration of laminated composite plates with temperature dependent properties by an asymptotic numerical method" *Int. J for Computational Methods in Engineering Science and Mechanics,* 43-57

5. Al-Waily, M, Jweeg, M and Al-Shammari, M.A (2020) "An analytical investigation of thermal buckling behavior of composite plates reinforced by carbon nano particles" *Engg Journal*, **24** (3), 11-21

6. Babu, C.S. and Kant, T. (2000) "Refined higher order finite element models for thermal buckling of laminated composite and sand wich plates," *J. of Therm. Stresses*, **23**, 111-130.

7. Brischetto, S. (2009) "Effect of the through-the-thickness temperature distribution on the response of layered and composite shells," *Int J. of Appl Mechan*, Vol.**1** (4), 581-605.

8. Croll J.G.A and Wang, H (2017) "Lower bound buckling for design of laminate composite cylinders" *Int J for Computational Methods in Engg Sc and Mechanics*, **18** (1), 112-115

9. Challamel, N, kolvik, G and Hellesland, H (2013) "Plate buckling analysis using a general higher-order shear deformation theory" *Int J of structural stability,* **13** (5), 1350028 (1-26)

10. Dash, P.K., Sathisbabu, R. and Ganesan, C (2011). "Effect of corrosive environment on elasto-buckling strength of GFRC plate," *Asian. J of Mater. Sci.* 1-15

11. Jones, R. M. (2005) "Thermal buckling of uniformly heated unidirectional and symmetric cross-ply laminated fiber-reinforced composite uniaxial in-plane restrained simply supported rectangular plates," *Composites. Part A*. **36**, 1355-1367.

12. Kumar, S.K. and Singh, B .N. (2008) "Thermal buckling analysis of SMA fiber-reinforced composite plates using layerwise model," *J. Aero. Engg*. **53** (1), 1-7.

13. Kumar, P.P and Subbarao, V.V (2019) "First order shears deformation theory access for the stress research of cnt/polymer laminated composite plates" *Int J of Engg and Advanced Technology,* **8** (6), 3736-3740

14. Lal, A., Singh, B. N. and Kumar, R. (2009) "Effects of random system properties on the thermal buckling analysis of laminated composite plates," *Comput. and Struct.* **87**, 1119-1128.

15. Lal, A. and Singh, B. N. (2010) "Effect of uncertain system properties on thermo elastic stability of laminated composite plates under nonuniform temperature distribution," *Int J. of Appl Mechan,* **2** (2), 399-420.

16. Mutsunaga, H. (2007) "Free vibration and stability of angle-ply laminated composite and sandwich plates under thermal loading," *J. Compo. Struct.*, **77** (2), 249-262.

17. Osman, M.Y and Suleiman, O.M.E, (2017) "Buckling analysis of thin laminated composite plates using finite element method, *Int J. of engineering and advanced Technology*, **3** (3), 1-18

18. Patel, B.P., Ganapathi, M. and Makhecha, D. P. (2002) "Hygrothermal effects on the structural behavior of thick composites using higher-order theory," *Compo. Structs.* **56**, 25-34.

19. Pandey, R., Upadhaya, A.K. and Shukla, K.K. (2010), "Hygrothermoelastic postbuckling response of laminated composite plates," *J. of Aeros. Engin*. 23, 1-13.

20. Rhead, T.A, Butler,R and Hunt, W.G (2017) " Compressive strength of composite laminates with delamination induced with interaction of panel and sub-laminate buckling modes" *Composite Structures*, **171**, 326-334

21. Shojaee T, Mohammadi, B and Madoliat, R (2019) "Postbuckling analysis of laminated composites with cutout using experimental, numerical, and finite strip methods" *Modares Mechanical Engineering,* **19** (8) 2067-2077

22. Sai Ram, K.S. and Sinha, P.K. (1992) "Hygrothermal effects on the buckling of laminated composite plates," *Compo. Struct.* **21**, 233-247

23. Singh. S. K and Chakrabarti, A. (2012) "Buckling analysis of laminated composite plates using an efficient C^0 FE model, *Latin American J of Solids and Structures,* **1,** 1-13

24. Singh, B.N. and Verma, V.K. (2008) "Hygrothermal effects on the buckling of laminated composite plates with random geometric and material properties," *J of Reinf. Plast. and Compo.* **28**, 409-427.

25. Spallino, R. and Thierauf, G. (2000) "Thermal buckling optimization of composite laminates by evolution strategies," *Cmput. and Struct.***78**, 691-697.

26. Shariyat, M. (2007) "Thermal buckling analysis of rectangular composite plates with temperature-dependent properties based on a layer wise theory," *Thin-wall. Struc.* **45**, 439-452.

27. Shen-H-S. (2000) "Hygrothermal effects on the post buckling of shear deformable laminated plates," *Comput. Struct.* **53** (5), 1193-1204.

28. Torabizadeh, M.A, (2015) "Buckling of the composite laminates under mechanical loads with different layups using different plate theories" *Advanced Composites Letters,* **24** (1), 12-20

29. Xiao, S. and Chen, B. (2005) "Dynamic and buckling analysis of a thin elastic-plastic square plate in a uniform temperature field," *Acta. Mech. Sinic* .**21**, 181-186.

30. Zenkour, A.M. and EL-Sheikh, K. (2001) "Buckling and free vibration of elastic plates using simple and mixed shear deformation theories," Acta. Mecha. **46**, 183-197.

31. Zenkour, A.M. (2010) "The effect of transverse shear and normal deformations of the thermo mechanical bending of functionally graded sandwich plates," *Int J. of Appl Mechan,* **1** (4), 667-707.